Veterinary Immunology and Immunopathology 278 (2024) 110853

Contents lists available at ScienceDirect

Veterinary Immunology and Immunopathology

journal homepage: www.elsevier.com/locate/vetimm

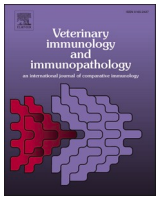

Solving technical issues in flow cytometry to characterize porcine CD8α/β expressing lymphocytes

Florian Ringl [a], Maria Stadler [b], Katinka A. van Dongen [a], Mahsa Adib Razavi [a], Armin Saalmüller [b], Kerstin H. Mair [a,b,*]

[a] Christian Doppler Laboratory for Optimized Prediction of Vaccination Success in Pigs, Immunology, Department of Biological Sciences and Pathobiology, University of Veterinary Medicine Vienna, Vienna, Austria
[b] Immunology, Department of Biological Sciences and Pathobiology, University of Veterinary Medicine Vienna, Vienna, Austria

ARTICLE INFO

Keywords:
Flow cytometry
Swine
CD8
Antibody clones
Steric inhibition

ABSTRACT

The CD8 molecule is a cell surface receptor and well described as co-receptor on T cells, binding directly to the major histocompatibility complex class I on antigen presenting cells. CD8 antigens are comprised of two distinct polypeptide chains, the α and the β chain. In the pig, the CD8 receptor is expressed by several lymphocyte subsets, including Natural Killer cells, γδ T cells and antigen experienced $CD4^+$ αβ T cells. On these cell populations CD8 is expressed as αα homodimers. Porcine cytolytic T cells on the other hand exclusively express CD8 αβ heterodimers. Several monoclonal antibodies (mAbs) for either of the two chains are available and are frequently used in flow cytometry. We observed that distinct combinations of mAb clones for CD8α and CD8β chains can cause troubles in multi-color staining panels. Therefore, we aimed for an in-depth study of the usage of different CD8-specific mAb clones and optimizing co-staining strategies for flow cytometry. We tested mAb clones 11/295/33 and 76–2–11 for the detection of CD8α and mAb clones PPT23 and PG164A for the detection of CD8β. The results indicate that the CD8α clone 11/295/33 should not be used together with either of the two CD8β clones in the same incubation step, as co-staining led to a highly reduced ability of CD8β mAb binding and loss in signal in flow cytometry. This can lead to potential false results in detecting CD8αβ cytolytic T cells. In case of the CD8α mAb clone 76–2–11, no inhibition in binding of either CD8β mAb clones was observed, making it the preferred choice in multi-color staining panels. The obtained data will help in future panel designs for flow cytometry in the pig and therefore improving studies of porcine immune cells.

1. Introduction

Studying the porcine immune system is gaining more importance, as this veterinary species is not only a valuable meat supplier but also an important model animal for research in human studies (Lunney et al., 2021). Different leukocyte subpopulations interplay in immune responses and are responsible to maintain physiological steady-state conditions and are activated in the case of infection or after immunization. To gain more insight into the phenotype and function of these diverse subpopulations, their characterization in immunological assays like flow cytometry (FCM) is crucial.

One of the markers to identify diverse immune-cell subsets is the surface glycoprotein CD8. The receptor consists of two amino acid chains, which are held together by disulfide bonds. For interaction with the major histocompatibility complex (MHC), the polypeptide chains possess a single immunoglobulin-like domain on the extracellular side of the receptor (Cole et al., 2012). CD8 interacts with the associated α3 domain of the MHC-class-I complex and therefore acts as a coreceptor of the T-cell receptor (TCR) which itself recognizes the epitope presented on MHC-class-I molecules (Devine et al., 1999). The CD8 molecule can be expressed in two different isoforms. Typically, it is expressed in the form of an αβ heterodimer, consisting of an α and a β chain. The other variant is the expression of an αα homodimer consisting of two identical α chains (Terry et al., 1990; Saalmüller et al., 1994). The monomer structure in the pig has a molecular weight of 33–35 kDa, while the dimer has a molecular weight of 66–70 kDa (Jonjić and Koszinowski, 1984; Pescovitz et al., 1984).

The CD8 receptor is expressed by several lymphocyte subsets in the pig, including $CD4^-$ αβ T cells, antigen-experienced $CD4^+$ αβ T cells, γδ T cells, and NK cells. Porcine $CD4^-CD8^+$ αβ T cells are also referred to as

* Corresponding author at: Immunology, Department of Biological Sciences and Pathobiology, University of Veterinary Medicine Vienna, Vienna, Austria.
E-mail address: Kerstin.Mair@vetmeduni.ac.at (K.H. Mair).

https://doi.org/10.1016/j.vetimm.2024.110853
Received 24 July 2024; Received in revised form 13 October 2024; Accepted 21 October 2024
Available online 22 October 2024

cytolytic T cells (CTL) and exclusively express CD8 αβ heterodimers (Gerner et al., 2009). They represent a very important type of immune cells and are characterized by the recognition of foreign antigens in an MHC-class-I restricted manner. On the other mentioned cell populations, CD8 is expressed as an αα homodimer (Yang and Parkhouse, 1997). Especially the existence of extrathymic T cells expressing both CD4 and CD8 is a peculiarity of swine (Saalmüller et al., 1987). Porcine $CD4^+CD8^-$ αβ T cells are referred to as naïve T helper cells as they have not yet had contact with foreign antigens. After antigen contact, they begin to proliferate and upregulate expression of CD8 molecules. Therefore, CD8 expression on $CD4^+$ T cells marks antigen-experienced cells and is a suitable tool to differentiate $CD4^+CD8^+$ memory from $CD4^+CD8^-$ naïve Th cells (Saalmüller et al., 2002). Furthermore, CD8α together with CD27 can be used to distinguish central and effector memory cells in the pig (Reutner et al., 2013). The γδ T cells are one of the major T-cell subpopulations in the peripheral blood lymphocytes (PBL) of pigs (Saalmüller et al., 1990; Yang and Parkhouse, 1996; Talker et al., 2013). The phenotypic classification is based on the division into $CD2^+$ and $CD2^-$ γδ T cells. Due to CD8 expression, the $CD2^+$ γδ T cells can be divided in two additional subgroups ($CD2^+CD8^-$ and $CD2^+CD8^+$ γδ T cells) with different functional properties (Stepanova and Sinkora, 2013; Kim et al., 2021). They likewise express the CD8 receptor in the form of an αα homodimer (Yang and Parkhouse, 1997). Phenotyping of porcine NK cells can only be made possible by specific marker combinations. Initially, porcine NK cells were defined by specific marker combinations and were described by a perforin$^+$CD2$^+$CD3$^-$CD4$^-$CD5$^-$CD6$^-$CD8α$^+$CD8β$^-$CD16$^+$ phenotype (Denyer et al., 2006) as individual selective markers are still missing. Phenotyping furthermore confirmed that porcine NK cells only express the CD8 receptor molecule in the form of CD8α homodimers (Denyer et al., 2006). More recently, it was described that porcine NK cells can be divided into distinct functional subsets based on different expression levels of the activating receptor NKp46 and CD8α (Mair et al., 2013).

This is highlighting that CD8 is an important molecule not only to discriminate porcine lymphocyte subpopulations, but also to distinguish subsets of diverse differentiation/ activation states. Several monoclonal antibodies (mAbs) for either of the two chains are available. Certain mAb clones are known that can recognize different epitopes on the CD8α or CD8β chain (Saalmüller et al., 1994; Dawson and Lunney, 2018). An important question is, if and how different CD8-specific mAbs can be combined in staining panels. An issue that becomes more important when opting for multi-color staining panels to address different lymphocyte subsets in a single sample. We observed obstacles when combining certain mAb clones directed against the CD8α and the CD8β chain in the same staining sample. In particular, the CD8β signal was diminished in certain mAb combinations, pointing towards inhibitory effects when using the anti-CD8α clone 11/295/33. Therefore, in this methodological study we aimed to investigate interactions of different mAb tools to optimize FCM panels in the pig.

2. Material and methods

2.1. CD8 transfected HEK293T cells

For testing of CD8α and CD8β mAb binding, recombinant fusion proteins of porcine CD8α with a N-terminal FLAG-tag, or CD8β with a C-terminal 6His-tag were generated and expressed in HEK293T cells. RNA extraction and cDNA synthesis of lymphocytes isolated from porcine PBMCs was done as described (Lagler et al., 2019). For PCRs, gene-specific primers with restriction overhangs were designed (Supplementary Table 1). Amplification was performed using a proof-reading polymerase (S7 Fusion High-Fidelity DNA Polymerase, Biozym Scientific GmbH, Hessisch Oldendorf, Germany), with optimized primer annealing temperatures and elongation times for the respective amplicons following standard protocols (Supplementary Table 2). Purified PCR products were sub-cloned by blunt-end cloning (pJET1.2/blunt cloning vector, Thermo Fisher Scientific, Vienna, Austria) according to manufacturer's protocol. For generating final expression constructs, subcloned inserts were ligated into pSF-CMV-NH2-PPT-3xFLAG® N-terminal FLAG-tag mammalian expression vector (Sigma-Aldrich, Vienna, Austria) using restriction enzymes for *Eco*RI and *Eco*RV (Thermo Fisher Scientific) for CD8α, or pSF-CMV-Puro-COOH-TEV-6His (OG1122) C-terminal 6His-tag mammalian expression vector (Sigma-Aldrich) using restriction enzymes for *Eco*RV and *Xho*I (Thermo Fisher Scientific) for CD8β, with standard procedures for sticky-end cloning. Sequences and in-frame cloning of constructs were confirmed by sequencing (Eurofins Genomics, Ebersberg, Germany). After propagation of HEK293T cells in DMEM supplemented with 1 mM sodium pyruvate, 100 U/mL penicillin, 0.1 mg/mL streptomycin (all PAN-Biotech, Aidenbach, Germany) and 10 % heat-inactivated FBS (Gibco™, Thermo Fisher Scientific), 1.6×10^6 cells were seeded into 25 cm^2 cell culture flasks. At 70–80 % confluency, cells were transfected with PolyFect® transfection reagent (Qiagen, Hilden, Germany) according to manufacturer's instructions. For detachment of adherent cells, Trypsin–EDTA (PAN-Biotech) was applied. Cells were analyzed by FCM 24 hours after transfection alongside non-treated HEK293T cells as negative control. The FCM staining procedure is described in more detail below and antibodies used are outlined in Table 1.

2.2. Animals and cellular material

The samples of porcine blood for the isolation of lymphocytes needed for the experiments were obtained from six-to-seven months old healthy pigs from a slaughterhouse. Animals underwent electric high-voltage anesthesia and subsequent exsanguination in accordance with the Austrian Animal Welfare Slaughter Regulation. Whole blood was collected in beakers with heparin solution. Peripheral blood mononuclear cells (PBMCs) were isolated by gradient centrifugation using lymphocyte separation medium (Pancoll, 1.077 g/mL, PAN Biotech). Samples were frozen at −150°C for future use. For experiments we performed previous tests with fresh as well as frozen material. As no adverse effects were observed with frozen material, this was chosen for further experiments.

2.3. ELISA assays

Plates were coated with CD8 peptides at 10 μg per well, designed as 15-mers with five amino-acids overlap (Intavis peptide services, Tübingen, Germany) overnight at 4°C. Used peptides are listed in Supplementary Tables 3 and 4. After blocking with PBS supplemented with 1 % bovine serum albumin (w/v, PAN Biotech) for one hour at room temperature (RT), anti-CD8 antibodies were applied for two hours at RT with undiluted cell culture supernatants for clones 11/295/33, 76–2–11, and PPT23, and 250 ng per well for clone PG164A. Detection was conducted with goat anti-mouse IgG-Biotin (Jackson Immuno Research) for 1.5 hours, and Streptavidin conjugated with horseradish peroxidase (Roche, Vienna, Austria) for one hour, followed by tetramethylbenzidine substrate for 30 min. As control for unspecific binding the same setups without the specific anti-CD8 mAbs were used. All washing steps were performed with PBS (PAN Biotech) supplemented with 0.02 % Tween 20 (Sigma-Aldrich). Samples were analyzed on an ELISA plate reader (Magellan™ standard V7.2, Tecan, Männedorf, Switzerland) at a wavelength of 450 nm.

2.4. Flow cytometry

Cells were stained in 96-well round-bottom plates. All main incubation steps were performed for 20 min at 4°C in the dark. Each incubation step was followed by two washing steps in buffer (4 min, 4°C, 470 g). For HEK293T cells, PBS supplemented with 3 % (v/v) FBS was used as staining buffer, while for porcine PBMCs, PBS supplemented with 10 % (v/v) porcine plasma (in-house preparation) was used. For

Table 1
Primary antibodies and secondary reagents used for FCM analyses.

Antigen	Clone	Isotype	Fluorochrome	Labeling strategy	Source of primary Ab
Transfected HEK293T cells					
CD8α	11/295/33	IgG2a	Alexa647	directly conjugated[a]	in-house
CD8α	295/33–25	IgG2a	PE	directly conjugated	BD Biosciences[b]
CD8α	76–2–11	IgG2a	PE	directly conjugated	BD Biosciences
CD8β	PPT23	IgG1	BV421	secondary antibody[c]	in-house
CD8β	PG164A	IgG2a	BV421	secondary antibody[d]	Kingfisher Biotech[e]
FLAG	M2	IgG1	BV421	secondary antibody[c]	Sigma-Aldrich
6xHis tag	polyclonal	rb IgG	FITC	directly conjugated	Abcam[f]
CD8α and CD8β co-staining					
CD3	BB23–8E6	IgG2b	Alexa488	secondary antibody[g]	Southern-Biotech[h]
CD3	BB23–8E6	IgG2b	BV421	secondary antibody[i]	Southern-Biotech
CD8α	11/295/33	IgG2a	Alexa647	secondary antibody[j]	in-house
CD8α	11/295/33	IgG2a	Alexa488	directly conjugated[k]	in-house
CD8α	76–2–11	IgG2a	Alexa647	secondary antibody[j]	in-house
CD8α	76–2–11	IgG2a	PE	directly conjugated	BD Biosciences
CD8β	PPT23	IgG1	BV421	secondary antibody[c]	in-house
CD8β	PG164A	IgG2a	Alexa647	directly conjugated[a]	Kingfisher Biotech
CD8α and CD8β mAb blocking					
CD8α	11/295/33	IgG2a	w/o		in-house
CD8α	11/295/33	IgG2a	Alexa647	directly conjugated[a]	in-house
CD8α	76–2–11	IgG2a	w/o		in-house
CD8β	PPT23	IgG1	w/o		in-house
CD8β	PPT23	IgG1	Alexa488	secondary antibody[l]	in-house
CD8β	PPT23	IgG1	Alexa488	directly conjugated[k]	in-house
CD8β	PG164A	IgG2a	Alexa647	directly conjugated[a]	Kingfisher Biotech
CD8α and CD8β peptide blocking					
CD3	BB23–8E6	IgG2b	Alexa488	secondary antibody[g]	Southern-Biotech
CD8α	11/295/33	IgG2a	Alexa647	secondary antibody[j]	in-house
CD8α	76–2–11	IgG2a	Alexa647	secondary antibody[j]	in-house
CD8β	PPT23	IgG1	Alexa647	secondary antibody[m]	in-house
CD8β	PG164A	IgG2a	Alexa647	secondary antibody[j]	Kingfisher Biotech

[a] Alexa Fluor 647 conjugation kit, Thermo Fisher Scientific;
[b] BD Biosciences, San Jose, CA, USA;
[c] rat-anti mouse IgG1-Brilliant Violet 421, BioLegend, San Jose, CA, USA;
[d] goat anti-mouse IgG2a-Brilliant Violet 421, Jackson Immuno Research, Suffolk, UK;
[e] Kingfisher Biotech, Saint Paul, MN, USA;
[f] Abcam, Cambridge, UK;
[g] goat anti-mouse IgG2b-Alexa Fluor 488, Jackson Immuno Research;
[h] Southern Biotech, Birmingham, AL, USA;
[i] goat anti-mouse IgG2b-Brilliant Violet 421, Jackson Immuno Research;
[j] goat anti-mouse IgG2a-Alexa Fluor 647, Jackson Immuno Research;
[k] Alexa Fluor 488 conjugation kit, Thermo Fisher Scientific;
[l] goat anti-mouse IgG1-Alexa Fluor 488, Thermo Fisher Scientific;
[m] goat anti-mouse IgG1-Alexa Fluor 647, Thermo Fisher Scientific

discrimination of dead cells, fixable viability dye eFluor780 was used according to manufacturer's protocol (Thermo Fisher Scientific). Samples were measured on a CytoFLEX LX (Beckman Coulter, Krefeld, Germany) and the final analysis, as well as the graphical display, was accomplished with the software FlowJo (Becton Dickinson Biosciences, USA, version 10.10.0). At least 1×10^5 cells were recorded per sample. For data analysis, an overall gating strategy was used. In the first step, cells were selected according to their sideward and forward scatter properties (SSC-A and FSC-A). Subsequently, cell doublets were excluded (FSC-A/FSC-H), followed by exclusion of dead cells by gating on viability dye negative cells (Supplementary Figure 1 A and 1B for HEK293T cells or porcine lymphocytes, respectively).

2.4.1. *CD8α and CD8β co-staining assays*

The aim was to examine the binding of the anti-CD8β clones by adding the anti-CD8α clones at different timepoints in the staining panels on porcine lymphocytes. The first group analyzed was the control group (without anti-CD8α mAbs). In the second group anti-CD8α mAbs were added simultaneously with the anti-CD8β mAbs. The third group included the addition of the anti-CD8α mAbs 20 minutes (one incubation step) before the addition of the anti-CD8β mAbs. This process was also measured the other way round for the fourth group. In the last group, the anti-CD8α mAbs were added to the anti-CD8β mAbs with a delay of five minutes. As co-staining, the pan T-cell marker CD3 was selected. Used antibodies are outlined in Table 1.

2.4.2. *CD8α and CD8β mAb blocking assays*

For the FCM blocking assays, different amounts of the blocking antibody were used (10x, 1x, 0.1x, and 0.01x of the optimal amount for FCM, defined by previous titrations) on porcine lymphocytes. This was followed by addition of the mAb clone to be blocked in optimal titrated amounts. The following combinations were tested: CD8α/CD8α, CD8β/CD8β, and CD8α/CD8β mAb clones. Used antibodies are outlined in Table 1.

2.4.3. *CD8α and CD8β peptide blocking assays*

To test for the potential blocking on the binding of anti-CD8 mAb clones, mAbs were incubated with corresponding peptides as described in 2.3 for one hour. Peptide-blocked mAbs were then added to porcine lymphocytes and staining was performed as described above. As control,

mAbs incubated with DMSO only in the same concentration as used for peptide dissolving was applied. As co-staining, the pan T-cell marker CD3 was selected. Used antibodies are outlined in Table 1 and used peptides are listed in Supplementary Tables 3 and 4.

2.5. Statistical analysis

Graphs were created with GraphPad PRISM (GraphPad Software, San Diego, CA, USA, version 10.2.3). Data was analyzed for statistical significance by SPSS® (SPSS Statistics Version 20.0, IBM Corp., Armonk, NY, USA). Obtained values were tested for normal distribution by the Kolmogorov-Smirnov test. All datasets met the requirement of normal distribution and were analyzed by ANOVA with Bonferroni correction as post-hoc analysis. Levels of significance were defined as: $p \leq 0.05$, $p \leq 0.01$, and $p \leq 0.001$. Within graphs, different letters indicate any significant differences that were observed.

3. Results

3.1. CD8 mapping on transfected cells

In a first step we wanted to verify binding of different mAb clones to porcine CD8α or CD8β chains. HEK293T cells were transiently transfected with either recombinant porcine CD8α to confirm CD8α-specific mAb clones or CD8α+β to test for CD8β mAb clones. The latter was selected as the β chain was reported to need the α chain for correct surface expression (Hennecke and Cosson, 1993). MAb clones 11/295/33 and 76–2–11 clearly stained CD8α only transfected cells, similar to CD8α+β transfected cells, thus confirming their binding on the CD8α chain (Fig. 1A). This was further supported by a co-staining with the anti-FLAG control antibody. In addition, staining with mAb clone 295/33–25 was performed. This mAb clone is regularly classified as "CD8b" similarly to clone 11/295/33. Nonetheless, this is rather referring to binding to the b epitope on the CD8α chain and not on the CD8β chain (Saalmüller et al., 1994; Zuckermann et al., 1998; Dawson and Lunney, 2018) - which was confirmed in our experiments as the mAb was binding also to the CD8α only transfected cells (Fig. 1A). On the other hand, mAbs designated to bind to the CD8β chain like PPT23 and PG164A, only showed a staining on CD8α+β transfected cells and not on the CD8α only transfected cells (Fig. 1B). This was further supported by co-staining with the anti-6His control antibody. Untransfected HEK293T cells served as negative control, where no staining was observed with any of the tested mAb clones.

3.2. Binding interferences shown in CD8α and CD8β co-staining experiments

When using distinct anti-CD8 mAb combinations in multi-color staining panels in FCM, we observed binding interferences, leading in a diminished signal of CD8β (Supplementary Figure 2). Therefore, we performed several experiments to investigate the interactions between different CD8α and CD8β binding mAb clones. The experiments were performed with samples of at least five different animals. Inhibitory effects on CD8β were shown in means of FCM signal changes depending on the time of addition of the respective CD8α binding mAb clones.

First, the effects of a co-staining with the anti-CD8α mAb clone 11/295/33 on the anti-CD8β PPT23 mAb clone were evaluated (Fig. 2A-C). The aim was to examine the binding of the PPT23 clone by adding the anti-CD8α mAbs at different timepoints in the staining procedure (color-coded groups) and to evaluate the resulting population size and signal strength caused by the CD8β-binding PPT23 mAb clone. As co-staining, the pan T-cell marker CD3 was used. The first group analyzed was the control group (w/o, red boxplots) and showed a staining with the PPT23 clone only, without CD8α mAbs. In the next group, anti-CD8α mAbs were added in the same incubation step as the PPT23 clone (simultaneous, SIM, orange boxplots). The third group included the addition of anti-CD8α mAbs one incubation step (20 minutes) before the addition of the PPT23 clone (alpha before, AB, green boxplots). This process was also measured in a reverse order, where the PPT23 clone was added 20 minutes before (alpha after, AA, light blue boxplots). In the last group, the anti-CD8α mAbs were added to the PPT23 clone in the same incubation step, but with a delay of only five minutes (alpha delayed,

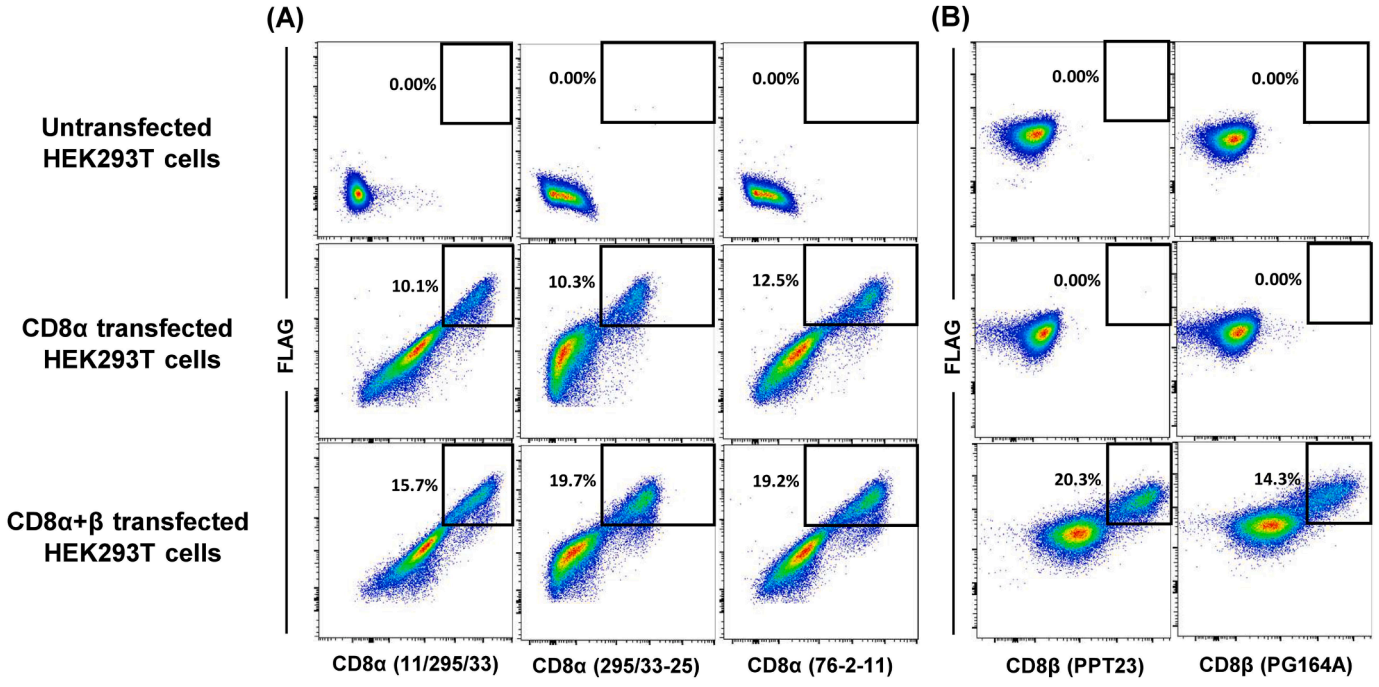

Fig. 1. CD8α and CD8β binding specificities on transfected cells. HEK293T cells without expression construct (upper row), transfected with porcine CD8α (middle row), or CD8α+β (bottom row) were tested for binding of (A) CD8α mAb clones 11/295/33, 295/33–25, and 76–2–11, or binding of (B) CD8β clones PPT23 and PG164A. Control antibodies against (A) FLAG-tag or (B) 6His-tag were used in parallel. Gates indicate frequencies of positively co-stained cells.

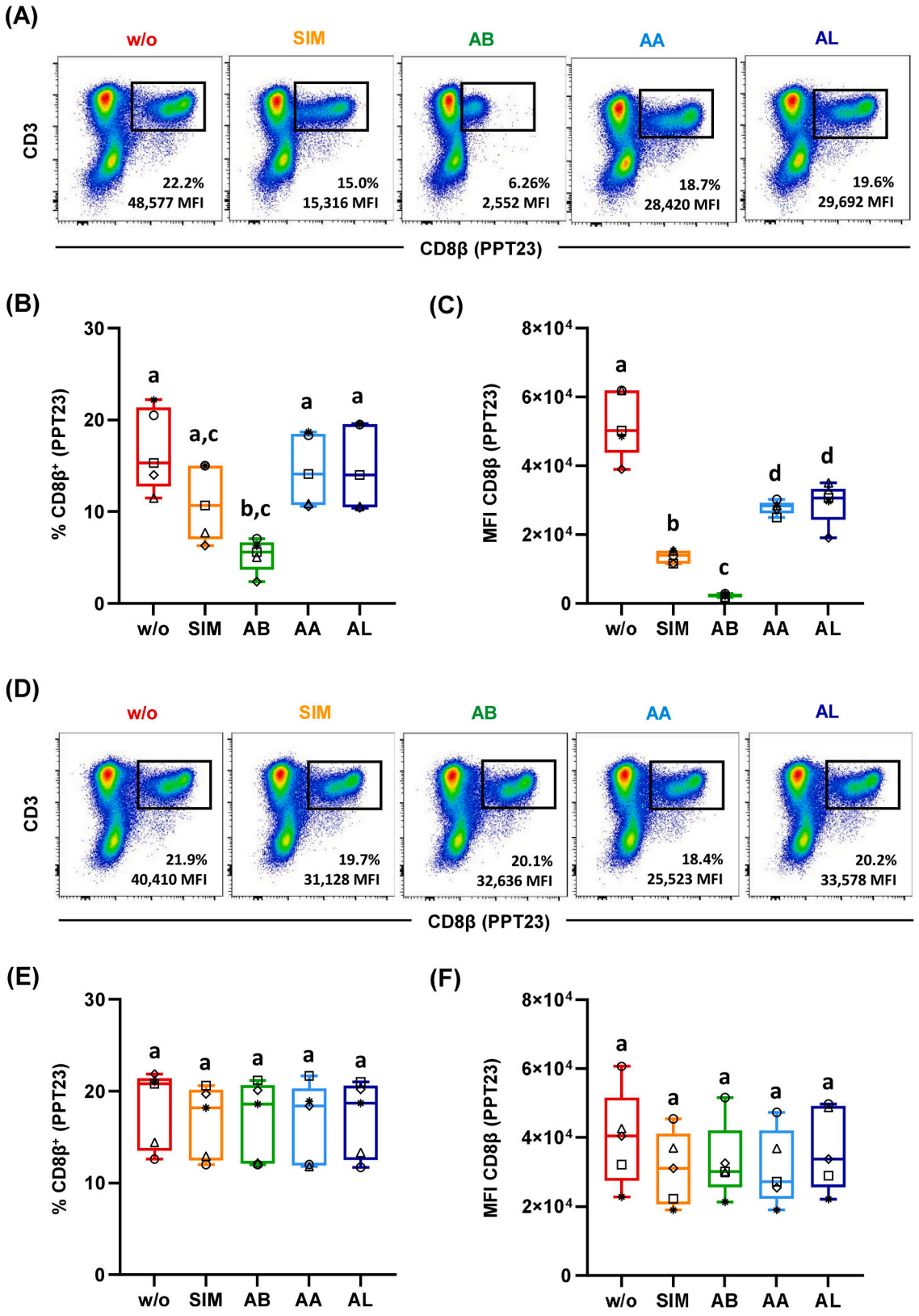

Fig. 2. Effects of different anti-CD8α mAbs on the binding of anti-CD8β mAb clone PPT23. The figure shows the effects of adding either the anti-CD8α 11/295/33 (A-C), or the anti-CD8α 76–2–11 mAb clones (D-F) to the anti-CD8β PPT23 mAbs at different timepoints (color-coded groups) in terms of the resulting CD8β signal strength. The pseudo-color plots represent the lymphocytes of a single representative animal (A, D). Frequencies and median fluorescence intensities (MFIs) are indicated in the gates. The experiment was performed with samples from five different animals. In the boxplots the frequencies of $CD8\beta^+$ lymphocytes (B, E) and the MFI of CD8β (C, F) are shown. Individual tested animals are represented by different symbols (animal represented by the asterisk shown in A, animal represented by the diamond shown in D). The middle line of each boxplot indicates the median of the tested animals for every group. Different letters indicate statistical differences between the groups.

AL, dark blue boxplots). The pseudo-color plots in Fig. 2A represent the lymphocytes of a single representative animal and display CD8β on the x-axis and CD3 on the y-axis. The $CD3^+CD8\beta^+$ cell populations are outlined in separate gates. The boxplots show the frequencies of $CD8\beta^+$ lymphocytes (Fig. 2B) and the median fluorescence intensity (MFI) of $CD8\beta^+$ cells (Fig. 2C) of all animals analyzed. We summarized results as median values of all animals analyzed in all following experiments. In contrast to the samples without the anti-CD8α mAb (w/o, %: 15.3 / MFI: 50,265), addition of the 11/295/33 clone caused a significant decrease in the resulting CD8β signal, as the frequencies and MFIs of $CD8\beta^+$ lymphocytes decreased with simultaneous (SIM, %: 10.7 / MFI: 13,978) and prior (AB, %: 5.6 / MFI: 2531) addition of CD8α mAbs. The addition of CD8α 11/295/33 mAbs 20 minutes after CD8β and the delayed addition after five minutes both resulted in similar percentages of $CD8\beta^+$ lymphocytes in comparison to the control group in every animal tested (AA: 14.1 %; AL: 14.0 %). The same trend was observed regarding the MFI of CD8β, although intensity could not be completely restored compared to the control group (AA: 28,420; AL: 30,607).

Next, the influence of the anti-CD8α mAb 76–2–11 on the binding of the anti-CD8β mAb PPT23 was investigated (Fig. 2D-F). The procedure was analogous to the first experiment and the results were presented in the same way as described above. From the pseudo-color plots, we concluded that the CD8β signal did not visibly change by the addition of the 76–2–11 mAb (Fig. 2D). The frequencies and MFIs of $CD8\beta^+$ lymphocytes were highest in the control group (w/o, %: 20.8 / MFI: 40,410) and did not significantly decrease in the different incubation groups with the 76–2–11 mAbs in all animals investigated (%: 18.2–18.7 / MFI: 27,204–33,758, Fig. 2E+F). In this experimental setup, it seemed that it had no significant influence at which time-point the 76–2–11 mAbs were added to the PPT23 mAbs.

The follow-up approach was to study the interactions between the anti-CD8α mAbs and anti-CD8β mAb clone PG164A (Fig. 3). Here we had to use directly labelled antibodies as all clones were of the same isotype. Starting with the anti-CD8α mAb 11/295/33, pseudo-color plots showed a strong decrease in the CD8β signal at each stage compared to the control group (Fig. 3A). The decrease compared to the control (w/o, %: 14.3 / MFI: 6974) was strongest when the 11/295/33 and the PG164A mAbs were added at the same time (SIM, %: 0.4 / MFI: 840) and when the 11/295/33 mAbs were added before the PG164A mAbs (AB, %: 1.2 / MFI: 992). Adding the 11/295/33 mAbs delayed by five minutes after the PG164A mAbs led to a greater decrease in PG164A binding success (AL, %: 1.8 / MFI: 915), than adding the 11/295/33 mAbs 20 minutes after the PG164A mAbs (AA, %: 5.6 / MFI: 1168, Fig. 3B+C).

The final experiment of this type involved studying the interactions between the anti-CD8α 76–2–11 mAbs and the anti-CD8β PG164A mAbs (Fig. 3D-F). When looking at the pseudo-color plots, it was noticeable that there was no clear difference between the $CD8\beta^+$ population of the control group and the $CD8\beta^+$ populations of the different co-staining groups (Fig. 3D). Regarding the percentage of $CD8\beta^+$ lymphocytes similar results were obtained for all groups tested (%: 16.5–18.0, Fig. 3E). In the box plots that display the MFI of CD8β, interestingly it was noticeable, that the control group had average lower values (w/o, MFI: 19,128), than the group in which the 76–2–11 mAbs were added about 20 minutes before the PG164A mAbs (AB, MFI: 30,286), although not statistically significant (Fig. 3F).

To investigate concentration-dependent influences, we further tested different amounts of anti-CD8α mAb 11/295/33 on CD8β clones PPT23 and PG164 A (Supplementary Figure 3). Even 10-times less of CD8α diminished the staining of CD8β (MFI PPT23: 3111; MFI PG164A: 2241), compared to values without CD8α (MFI PPT23: 11,246; MFI PG164A: 7942). Using 100-times less of CD8α was not enough to diminished the staining of CD8β.

3.3. Epitope mapping for CD8α and CD8β mAb clones

3.3.1. CD8α and CD8β blocking assays

The results so far showed that the intereference on CD8β binding only occurred when the CD8α mAb clone 11/295/33 was used, and not 76–2–11. Therefore, we wanted to investigate if the used anti-CD8 mAbs bind to different epitopes. The interactions between the CD8α or CD8β clones were examined in blocking assays. In each experiment, the effects of 10-fold, equal (1.0-fold), 0.1-fold and 0.01-fold amounts of one mAb (blocking) on the other mAbs were tested (Fig. 4).

First, cells were incubated with the anti-CD8α mAb 11/295/33 at different amounts. As positive control the same mAb clone was used in the second incubation step (Fig. 4A). The histogram overlays show the resulting CD8α signal. A clear reduction in the CD8α binding by means of reduced MFI signals was observed when blocking with high amounts of the same mAb (10x: 2182; 1x: 2771) compared to samples without blocking (8614), and even a slight reduction was observed with the 0.1x amount (5285). Similar effects were observed with 295/33–25 when blocking with 11/295/33 (Supplementary Figure 4), indicating that both mAbs bind to similar epitopes. Nonetheless, no blocking effect was observed when measuring signals for the 11/295/33 mAbs when blocking with the 76–2–11 mAbs in the same setting (Fig. 4B). Here, MFIs after blocking (9092−10,556) were similar to mAb staining without blocking (9285). The same setup was used to investigate CD8β mAbs. As positive control, PPT23 mAbs were used for blocking as well as for staining (Fig. 4C). Here again a reduction in the MFI signal was observed with high amounts of the same mAb (10x: 7581; 1x: 7748) compared to samples without blocking (14,300), although not statistically significant. No obvious differences were seen when using PG164A for blocking and PPT23 for staining (Fig. 4D, 79,079–115,624).

3.3.2. Epitope mapping by ELISA and flow cytometry

To determine the exact epitopes of the tested mAbs we used CD8α and CD8β specific peptides. For the anti-CD8α mAb 11/295/33 a distinct signal in ELISA was observed for peptides P5 (TVKLR CEVMH SNTLT) and P6 (SNTLT SCSWL YQKPG) with ODs of 0.57 and 0.41 (Fig. 5A), showing binding of the antibody to the peptide. No clear signals that could be allocated to a distinct peptide was seen for the mAb 76–2–11 (ODs for all peptides ≤ 0.06, Fig. 5B). Likewise, no distinct peptide could be identified for mAb clone PPT23 as the slightly elevated OD of 0.12 for P1 was also seen for P17 with an OD of 0.1 (Fig. 5C). A slightly pronounced signal was seen for the anti-CD8β mAb PG164A with an OD of 0.18 for P1 (Fig. 5D). As alternative strategy, peptides were used to block mAb binding sites before applying to flow cytometry staining of lymphocytes (Fig. 5E). If a distinct peptide was bound by the mAb, binding of the mAb to the CD8 molecule on lymphocytes was blocked. Here, we could confirm the blocking ability by P5, and especially P6 for CD8α mAb 11/295/33. P5 showed a reduction of 19 % of $CD8\alpha^+$ cells compared to the mAb without peptides (35.5 % vs. 43.7 %). P6 showed a reduction of 80 % of $CD8\alpha^+$ cells compared to the mAb without peptides (8.95 % vs. 43.7 %). For the other three mAb clones no positive results were obtained (data not shown), analogous to ELISA results.

4. Discussion

Certain anti-CD8 mAbs are known to recognize different epitopes on the CD8α chain, while others were reported to be specific for the CD8β chain (Haverson et al., 2001; Saalmüller et al., 1994, 1998; Yang and Parkhouse, 1997; Zuckermann et al., 1998). Several of those clones were generated by William C. Davis, to whom this special issue is dedicated.

Preliminary results from our group indicated that distinct combinations of mAbs for porcine CD8α and CD8β chains can cause troubles in multi-color staining panels which can lead to suboptimal detection of $CD8\beta^+$ cytolytic T cells. Therefore, aim of this methodological study was the in-depth investigation of the usage of different mAb clones for optimizing co-staining strategies. With this study we aimed to support

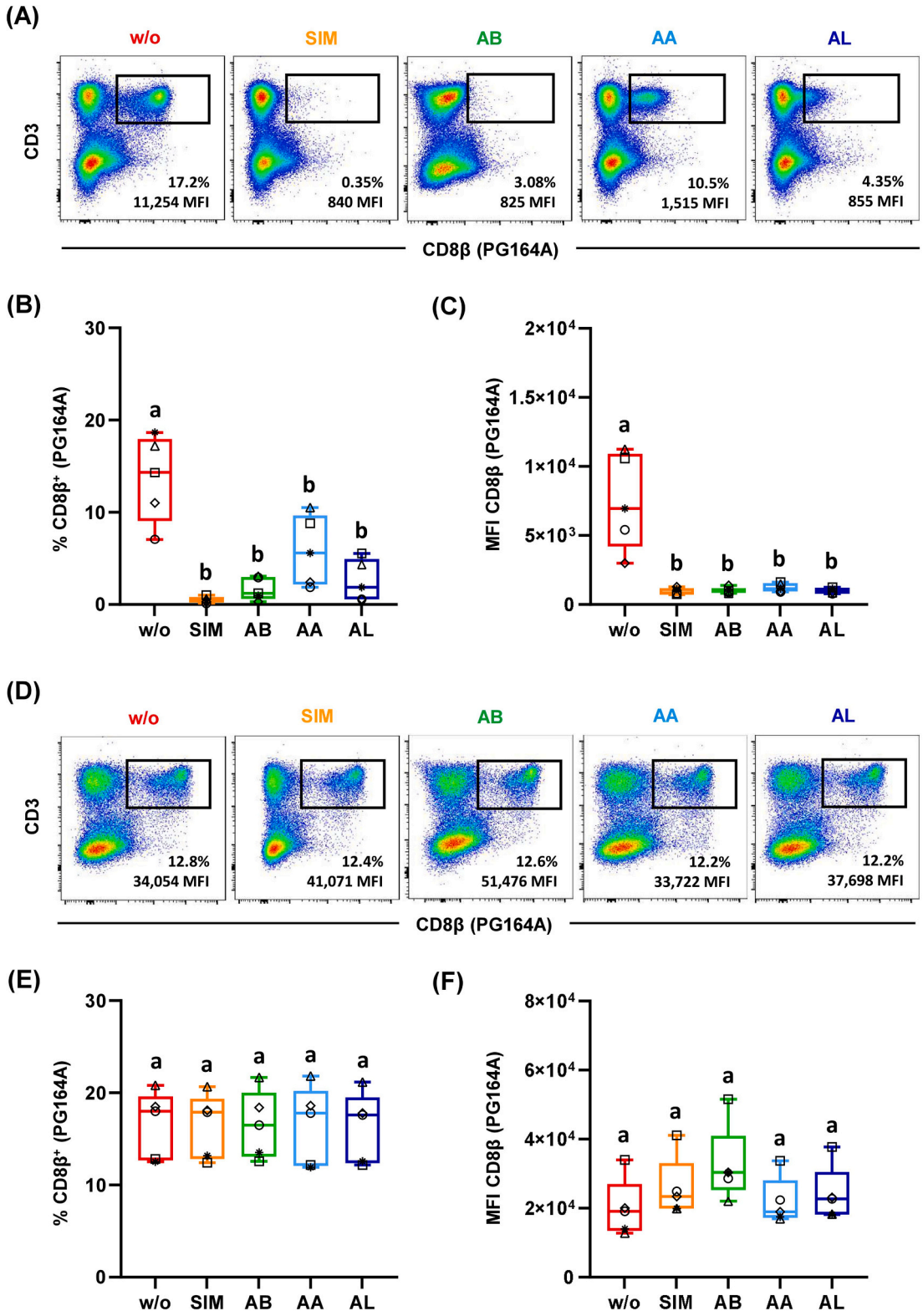

Fig. 3. Effects of different anti-CD8α mAbs on the binding of anti-CD8β mAb clone PG164A. The figure shows the effects of adding either the anti-CD8α 11/295/33 (A-C), or the anti-CD8α 76–2–11 mAb clones (D-F) to the anti-CD8β PG164A mAb clone at different timepoints (color-coded groups) in terms of the resulting CD8β signal strength. The pseudo-color plots represent the lymphocytes of a single representative animal (A, D). Frequencies and median fluorescence intensities (MFIs) are indicated in the gates. The experiment was performed with samples from five different animals. In the boxplots the frequencies of $CD8\beta^+$ lymphocytes (B, E) and the MFI of CD8β (C, F) are shown. Individual tested animals are represented by different symbols (animal represented by the triangle shown in A, animal represented by the square shown in D). The middle line of each boxplot indicates the median of the tested animals for every group. Different letters indicate statistical differences between the groups.

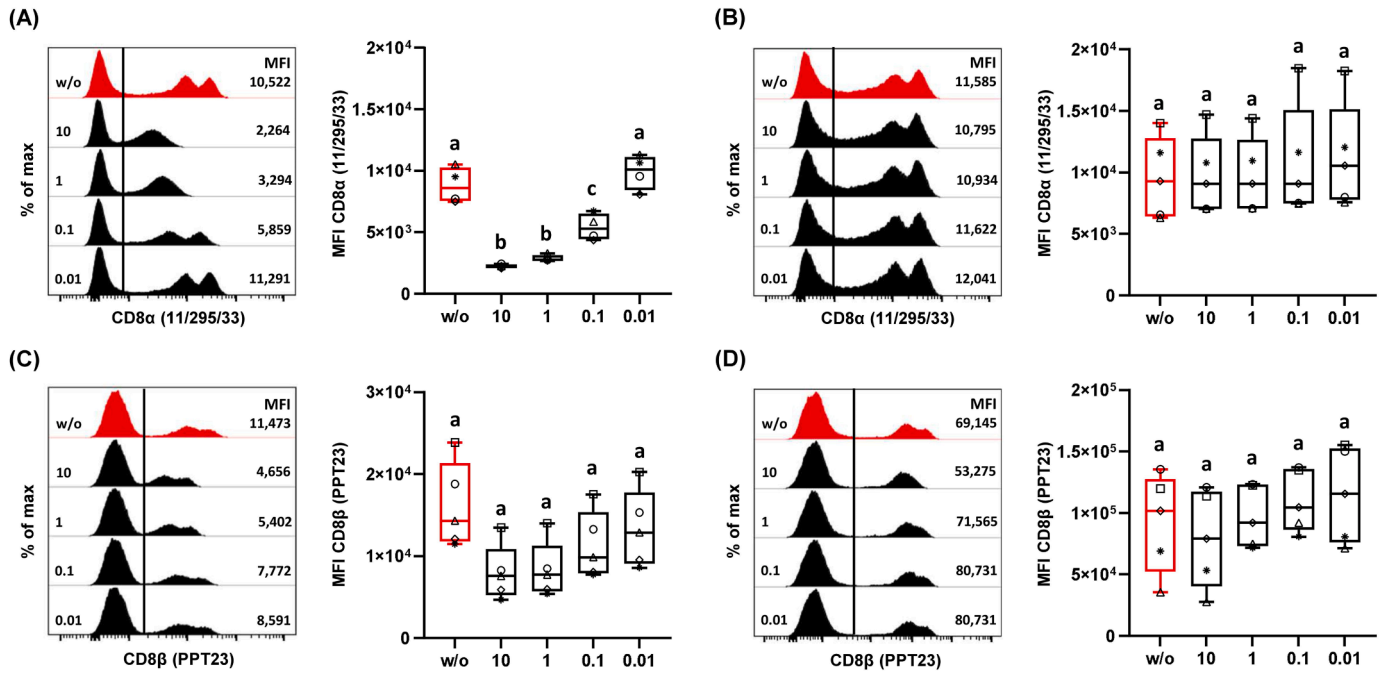

Fig. 4. Blocking assays with anti-CD8α and anti-CD8β mAb clones. The figure shows the effects of different amounts of previously added antibody (10x, 1x, 0.1x, 0.01x) in the context of blocking assays (black) and were compared to the tested mAb clone without any blocking (w/o, red). (A) Anti-CD8α mAb 11/295/33 was used for blocking and subsequent staining as positive control. (B) The effects on 11/295/33 staining after blocking with 76–2–11 is shown. (C) Anti-CD8β mAb PPT23 was used for blocking and subsequent staining as positive control. (D) The effects on PPT23 staining after blocking with PG164A is shown. Experiments were performed with samples from at least four different animals. The histogram overlay represents the lymphocytes of a single representative animal. The boxplots show the MFIs of CD8α or CD8β, respectively. The values of the individual tested animals are represented by different symbols (animal represented by the triangle shown in A, animal represented by the asterisk shown in B, animal represented by the asterisk shown in C, animal represented by the asterisk in D). The middle line of each boxplot indicates the median of the tested animals for every group. Different letters indicate statistical differences between the groups.

reagent selection and setups of multi-color staining panels. Experiments were performed with different mAbs for CD8α and CD8β chain detection in different FCM settings. We observed that staining with the 11/295/33 CD8α mAb generally had an inhibitory effect on the two CD8β mAbs PPT23 and PG164A, especially after pre-addition of the 11/295/33 mAbs 20 minutes before the tested CD8β mAbs. Applying the 11/295/33 mAbs after the CD8β mAbs seemed to improve the CD8β binding process to some extent, at least for the PPT23 mAbs.

The binding of an antibody to an antigen is generally referred to as antigen-antibody reaction. This reaction is reversible and represents a non-covalent interaction primarily based on electrostatic interactions, hydrogen bonds, van der Waals forces and hydrophobic interactions (Kapingidza et al., 2020). When multiple epitopes are in proximity, the binding of one antibody to a first epitope may spatially hinder the binding of another antibody to a second epitope (epitope masking). This happens when one antibody occupies a lot of space or takes up a position which might be unfavorable for other antibodies. A process that is known as steric hindrance (SH) or steric inhibition (Cowan and Underwood, 1988). Thus, antibodies binding to close epitopes may result in reduced binding of one of the antibodies, or even complete blocking of the binding (Cowan and Underwood, 1988; Matos, 2021). SH in the context of FCM can result in reduction or complete absence of detectable fluorescent signals. For that to happen, the antibodies must bind to the same molecule, or macromolecular complex and to spatially close epitopes (Matos, 2021; Shah et al., 2021). Matos et al. reported problems in the context of a diagnostic procedure of chronic lymphocytic leukemia. Here, steric hindrance was assumed to be the cause of the unexpected decrease in FCM fluorescence signal when using mAbs directed against different adjacent molecules on the cell surface (immunoglobulin kappa and lamda, CD19, and CD20). It was considered that anti-CD19 mAbs might interfere with the binding of anti-kappa and anti-lambda mAbs due to SH, because no kappa and lambda chain expression was detected on the surface of B cells when used in combination with CD19. It was concluded that the cause of this effect must be due to the spatial proximity between the CD19 protein and the transmembrane immunoglobulin molecules of the B-cell receptor (Matos, 2021). In our performed experiments, the binding of the 11/295/33 mAbs to their specific epitope on the CD8α chain probably obscures nearby epitopes on the CD8β chain and therefore make binding for the PPT23 and the PG164A mAbs difficult. As a result, we think that a possible local proximity of the antigen binding sites was the main cause for the observed CD8β signal loss in FCM. Regarding the 76–2–11 mAbs, no inhibitory effect on both CD8β mAbs could be reported.

As the 76–2–11 mAb binds to another epitope on the CD8α chain (Saalmüller et al., 1994 and shown by our blocking experiments), we assumed that it must be located farther away from the investigated epitopes on the CD8β chain and the epitope for the 11/295/33 mAbs. This was also shown in FCM blocking-based analyses in 1994 Saalmüller et al. In this experiment, six different mAb clones against porcine CD8 were used, including 11/295/33 and 76–2–11. Two different epitopes were defined, with 76–2–11 binding to epitope CD8a and 11/295/33 binding to epitope CD8b – both on the CD8α chain (Saalmüller et al., 1994). The same was observed for the two anti-CD8β mAbs in our blocking experiments. Although not leading to the identification of the distinct epitopes recognized by the single mAbs, these blocking experiments are useful to get a first idea of the epitope location and are used frequently in FCM for this purpose (Stein et al., 1993; Mair et al., 2012; Milburn et al., 2021).

Under these conditions, the two different epitopes for the PPT23 and the PG164A on the CD8β chain would have to be located very close to each other, since blocking of the 11/295/33 clone on both CD8β binding mAb clones was demonstrated. We could draw first conclusions by identifying the epitope for mAb clone 11/295/33. Nonetheless, proof for the distinct epitopes for the other mAb clones are still missing. As in

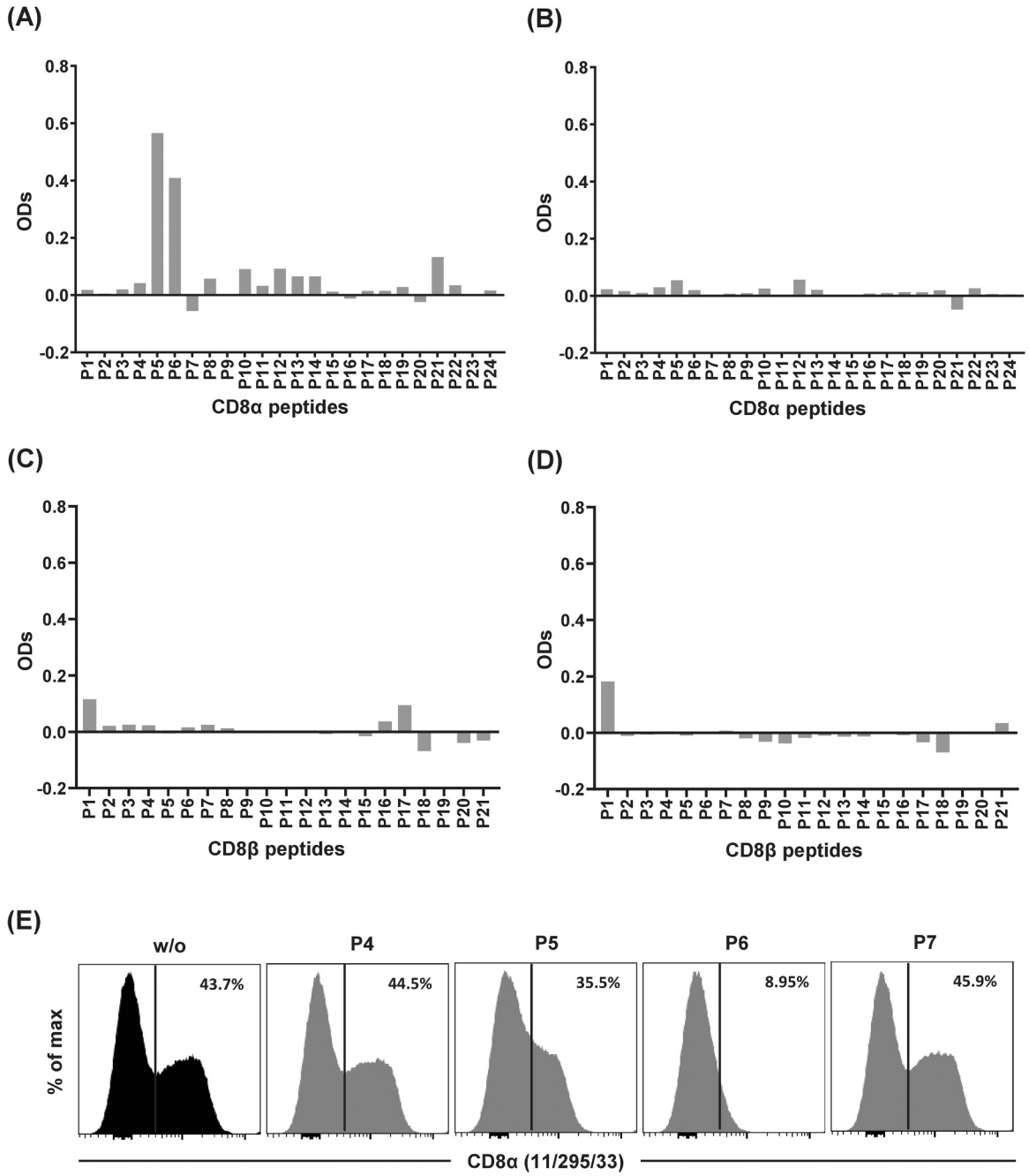

Fig. 5. Epitope mapping by ELISA and flow cytometry. CD8 peptides were used to investigate binding of distinct mAb clones to their distinct epitopes for (A) CD8α 11/295/33, (B) CD8α 76–2–11, (C) CD8β PPT23, and (D) CD8β PG164A in ELISA. Measured optical densities (ODs) are shown as result of CD8 mAb binding subtracted by unspecific binding of the secondary antibodies. (E) Results of FCM blocking assays with CD8α 11/295/33 are shown for selected peptides (P4-P7) compared to CD8 staining without peptides (w/o). Frequencies of positively stained cells are indicated.

ELISA only linear epitopes can be addressed (Abbott et al., 2014), we can conclude that the other mAbs might recognize conformational epitopes instead that are involved in SH.

The strength of a single binding interaction between antigen and antibody is described by the affinity. Antibodies with a higher affinity to their epitopes are more difficult to prevent from binding, than those with a low affinity (Khor et al., 2013; Kapingidza et al., 2020). Accordingly, a high affinity leads to a stronger and more stable labelling in FCM. If the affinity is rather low the bond is very unstable and is more easily be broken by several factors within the staining process. This might include the removal of antibodies by the washing process or the unsolicited displacement of an antibody by another due to a rather unstable binding or dependent on the mAb concentration (Abdiche et al., 2017). A lower affinity may therefore also add up to the observed loss in CD8β signals in our experiments. We assume that this was also the main cause for the generally observed increased MFI values of CD8β when the 76–2–11 mAbs were added before the PG164A mAbs, as here CD8β mAbs were added in the second incubation step, therefore undergoing one less washing step. The proposed epitope binding assays by Abdiche et al. might further shed more light if adjacent/minimally overlapping epitopes or different affinities are the major cause of the observed signal losses for CD8β (Abdiche et al., 2017).

To understand the exact mechanism of SH in the context of FCM, knowledge about the distribution of the molecules on the observed cell

surface and the exact localization of the epitopes are very useful. The underlying factors that eventually lead to blockade between antibodies are not clear and often vary widely. For example, the molecular weight of the competing fluorochromes (the combination of heavier molecules such as PE and PE-Cy5) was considered to be the causative factor for the occurrence of SH (Vita et al., 2015; Matos, 2021). The same could account when using indirect staining strategies. Further, immunolabelling in general was described to cause loss in antibody binding or hindrance in multiplexed staining (Hlavacek et al., 1999; Michele et al., 2016; Mello et al., 2021). To rule out this possibility, the experiment with the 11/295/33 and PPT23 mAb clones, likewise to the experiment with PG164A, was also repeated with directly stained mAbs, leading to the same results (data not shown). Also, the experiments in Supplementary Figure 3 were performed with unconjugated mAb clone 11/295/33.

It was also reported that the degree of membrane protrusions (e. g. microvilli) on the cell surface could contribute to preventing the binding of the reagent involved (Wang et al., 2014), a fact that is not applicable in out settings of PBMC staining. Furthermore, concentrations can effect antibody-antigen reaction (Reverberi and Reverberi, 2007). This was also addressed in Supplementary Figure 3, as different amounts of the CD8α mAbs were tested and also 10-times lower amounts showed the same effect.

Several approaches were proposed to minimize the effects of SH, if possible. First, any mAb combination used in the FCM process should be tested beforehand in comparison to single staining panels. The problem of SH can be the use of too high concentrations of the primary antibody. To determine the correct amounts of antibodies to be used in the FCM process, it is recommended to perform antibody titrations. However, unexpected antibody behavior may occur even when the staining procedure is part of an already validated protocol (Tangri et al., 2013; Vita et al., 2015; Shah et al., 2021). Or as we propose: to use another mAb clone if available.

In conclusion, the anti-CD8α 11/295/33 mAb clone should not be used simultaneously in the same staining step with the anti-CD8β PPT23 or the anti-CD8β PG164A mAb clone in an FCM staining panel, as this can lead to a reduction of the detectable FCM signal for CD8β and difficult interpretation of CTL results. Regarding the anti-CD8α 76–2–11 mAbs, no blocking effect on the CD8β binding mAbs could be reported, making 76–2–11 the preferable choice for detection of CD8α when planning multi-color staining panels including CD8β mAbs. This can be applied for future studies addressing CTLs (defined by the CD8β phenotype) in combination with lymphocyte subsets expressing the CD8α homodimers (like NK cells, γδ T cells, or $CD4^+$ antigen-experienced T cells).

Author contributions

FR and MS performed flow cytometry experiments. MS performed ELISA and blocking experiments. MAR was responsible for cloning of CD8 molecules. KAVD performed experiments on transfected cells and blocking experiments. KHM and AS were responsible for the conception and design of the study. FR and KHM analyzed the data and wrote the manuscript. All authors have read and approved the manuscript.

Funding

This work was supported by the Christian Doppler Research Association, Vienna, Austria, and Boehringer Ingelheim Vetmedica GmbH within the “Christian Doppler Laboratory for Optimized Prediction of Vaccination Success in Pigs.” The financial support by the Austrian Federal Ministry for Digital and Economic Affairs, the National Foundation for Research, Technology and Development, and the Christian Doppler Research Association is gratefully acknowledged. The funder was not involved in the study design, collection, analysis, interpretation of data, the writing of this article, or the decision to submit it for publication.

CRediT authorship contribution statement

Florian Ringl: Writing – original draft, Visualization, Methodology, Investigation, Formal analysis. **Maria Stadler:** Investigation. **Armin Saalmüller:** Writing – review & editing, Validation, Supervision, Conceptualization. **Kerstin H Mair:** Writing – review & editing, Writing – original draft, Visualization, Validation, Supervision, Investigation, Formal analysis, Conceptualization. **Katinka A van Dongen:** Methodology, Investigation. **Mahsa Adib Razavi:** Methodology, Investigation.

Declaration of Competing Interest

The authors declare that they have no known competing financial interests or personal relationships that could have appeared to influence the work reported in this paper.

Appendix A. Supporting information

Supplementary data associated with this article can be found in the online version at doi:10.1016/j.vetimm.2024.110853.

References

Abbott, W.M., Damschroder, M.M., Lowe, D.C., 2014. Current approaches to fine mapping of antigen-antibody interactions. Immunology 142, 526–535.
Abdiche, Y.N., Yeung, A.Y., Ni, I., Stone, D., Miles, A., Morishige, W., Rossi, A., Strop, P., 2017. Antibodies TArgeting Closely Adjacent Or Minimally Overlapping Epitopes Can Displace One another. PloS One 12, e0169535.
Cole, D.K., Laugel, B., Clement, M., Price, D.A., Wooldridge, L., Sewell, A.K., 2012. The molecular determinants of CD8 co-receptor function. Immunology 137, 139–148.
Cowan, R., Underwood, P.A., 1988. Steric effects in antibody reactions with polyvalent antigen. J. Theor. Biol. 132, 319–335.
Dawson, H.D., Lunney, J.K., 2018. Porcine cluster of differentiation (CD) markers 2018 update. Res. Vet. Sci. 118, 199–246.
Denyer, M.S., Wileman, T.E., Stirling, C.M.A., Zuber, B., Takamatsu, H.-H., 2006. Perforin expression can define CD8 positive lymphocyte subsets in pigs allowing phenotypic and functional analysis of natural killer, cytotoxic T, natural killer T and MHC un-restricted cytotoxic T-cells. Vet. Immunol. Immunopathol. 110, 279–292.
Devine, L., Sun, J., Barr, M.R., Kavathas, P.B., 1999. Orientation of the Ig domains of CD8 alpha beta relative to MHC class I. J. Immunol. 162, 846–851.
Gerner, W., Käser, T., Saalmüller, A., 2009. Porcine T lymphocytes and NK cells–an update. Dev. Comp. Immunol. 33, 310–320.
Haverson, K., Saalmüller, A., Alvarez, B., Alonso, F., Bailey, M., Bianchi, A.T., Boersma, W.J., Chen, Z., Davis, W.C., Dominguez, J., Engelhardt, H., Ezquerra, A., Grosmaire, L.S., Hamilton, M.J., Hollemweguer, E., Huang, C.A., Khanna, K.V., Kuebart, G., Lackovic, G., Ledbetter, J.A., Lee, R., Llanes, D., Lunney, J.K., McCullough, K.C., Molitor, T., Nielsen, J., Niewold, T.A., Pescovitz, M.D., La Lastra, J.M., de, Rehakova, Z., Salmon, H., Schnitzlein, W.M., Seebach, J., Simon, A., Sinkora, J., Sinkora, M., Stokes, C.R., Summerfield, A., Sver, L., Thacker, E., Valpotic, I., Yang, H., Zuckermann, F.A., Zwart, R., 2001. Overview of the third international workshop on swine leukocyte differentiation antigens. Vet. Immunol. Immunopathol. 80, 5–23.
Hennecke, S., Cosson, P., 1993. Role of transmembrane domains in assembly and intracellular transport of the CD8 molecule. J. Biol. Chem. 268, 26607–26612.
Hlavacek, W.S., Posner, R.G., Perelson, A.S., 1999. Steric effects on multivalent ligand-receptor binding: exclusion of ligand sites by bound cell surface receptors. Biophys. J. 76, 3031–3043.
Jonjić, S., Koszinowski, U.H., 1984. Monoclonal antibodies reactive with swine lymphocytes. I. Antibodies to membrane structures that define the cytolytic T lymphocyte subset in the swine. J. Immunol. 133, 647–652.
Kapingidza, A.B., Kowal, K., Chruszcz, M., 2020. Antigen-antibody complexes. Sub Cell. Biochem. 94, 465–497.
Khor, S.M., Thordarson, P., Gooding, J.J., 2013. The impact of antibody/epitope affinity strength on the sensitivity of electrochemical immunosensors for detecting small molecules. Anal. Bioanal. Chem. 405, 3889–3898.
Kim, S., Lim, B., Mattoo, S.-U.-S., Oh, E.-Y., Jeong, C.-G., Kim, W.-I., Lee, K.-T., Lee, S.-M., Kim, J.-M., 2021. Comprehensive transcriptomic comparison between porcine CD8- and CD8+ gamma delta T cells revealed distinct immune phenotype. Anim. Open Access J. MDPI 11.
Lagler, J., Mitra, T., Schmidt, S., Pierron, A., Vatzia, E., Stadler, M., Hammer, S.E., Mair, K.H., Grafl, B., Wernsdorf, P., Rauw, F., Lambrecht, B., Liebhart, D., Gerner, W., 2019. Cytokine production and phenotype of Histomonas meleagridis-specific T cells in the chicken. Vet. Res. 50, 107.
Lunney, J.K., van Goor, A., Walker, K.E., Hailstock, T., Franklin, J., Dai, C., 2021. Importance of the pig as a human biomedical model. Sci. Transl. Med. 13, eabd5758.
Mair, K.H., Essler, S.E., Patzl, M., Storset, A.K., Saalmüller, A., Gerner, W., 2012. NKp46 expression discriminates porcine NK cells with different functional properties. Eur. J. Immunol. 42, 1261–1271.

Mair, K.H., Müllebner, A., Essler, S.E., Duvigneau, J.C., Storset, A.K., Saalmüller, A., Gerner, W., 2013. Porcine CD8αdim/-NKp46high NK cells are in a highly activated state. Vet. Res. 44, 13.
Matos, D.M., 2021. Steric hindrance: a practical (and frequently forgotten) problem in flow cytometry. Cytom. Part B Clin. Cytom. 100, 397–401.
Mello, M.G., de, Westerhausen, M.T., Singh, P., Doble, P.A., Wanagat, J., Bishop, D.P., 2021. Assessing the reproducibility of labelled antibody binding in quantitative multiplexed immuno-mass spectrometry-imaging. Anal. Bioanal. Chem. 413, 5509–5516.
Michele, C., de, Los, Rios, P., de, Foffi, G., Piazza, F., 2016. Simulation and theory of antibody binding to crowded antigen-covered surfaces. PLoS Comput. Biol. 12.
Milburn, J.V., Hoog, A.M., Winkler, S., van Dongen, K.A., Leitner, J., Patzl, M., Saalmüller, A., Luca, K., de, Steinberger, P., Mair, K.H., Gerner, W., 2021. Expression of CD9 on porcine lymphocytes and its relation to T cell differentiation and cytokine production. Dev. Comp. Immunol. 121, 104080.
Pescovitz, M.D., Lunney, J.K., Sachs, D.H., 1984. Preparation and characterization of monoclonal antibodies reactive with porcine PBL. J. Immunol. 133, 368–375.
Reutner, K., Leitner, J., Müllebner, A., Ladinig, A., Essler, S.E., Duvigneau, J.C., Ritzmann, M., Steinberger, P., Saalmüller, A., Gerner, W., 2013. CD27 expression discriminates porcine T helper cells with functionally distinct properties. Vet. Res. 44, 18.
Reverberi, R., Reverberi, L., 2007. Factors affecting the antigen-antibody reaction. Blood Transfus. 5, 227–240.
Saalmüller, A., Aasted, B., Canals, A., Dominguez, J., Goldman, T., Lunney, J.K., Maurer, S., Pescovitz, M.D., Pospisil, R., Salmon, H., 1994. Analyses of mAb reactive with porcine CD8. Vet. Immunol. Immunopathol. 43, 249–254.
Saalmüller, A., Hirt, W., Reddehase, M.J., 1990. Porcine gamma/delta T lymphocyte subsets differing in their propensity to home to lymphoid tissue. Eur. J. Immunol. 20, 2343–2346.
Saalmüller, A., Pauly, T., Lunnery, J.K., Boyd, P., Aasted, B., Sachs, D.H., Arn, S., Bianchi, A., Binns, R.M., Licence, S., Whyte, A., Blecha, F., Chen, Z., Shu, R.M., Davis, W.C., Denham, S., Yang, H., Whittall, T., Parkhouse, R.M., Dominguez, J., Ezquerra, A., Alonso, F., Horstick, G., Howard, C., Sopp, P., Kim, Y.B., Lipp, J., Mackay, C., Magyar, A., Magyar, A., McCullough, K., Arriens, A., Summerfield, A., Murtaugh, M., Nielsen, J., Novikov, B., Pescovitz, M.D., Schuberth, H.J., Leibold, W., Schütt, C., Shimizu, M., Stokes, C., Haverson, K., Bailey, M., Tlaskalova, H., Trebichavsky, I., Valpotic, I., Walker, J., Lee, R., Zuckermann, F., 1998. Overview of the second international workshop to define swine cluster of differentiation (CD) antigens. Vet. Immunol. Immunopathol. 60, 207–228.
Saalmüller, A., Reddehase, M.J., Bühring, H.J., Jonjić, S., Koszinowski, U.H., 1987. Simultaneous expression of CD4 and CD8 antigens by a substantial proportion of resting porcine T lymphocytes. Eur. J. Immunol. 17, 1297–1301.
Saalmüller, A., Werner, T., Fachinger, V., 2002. T-helper cells from naive to committed. Vet. Immunol. Immunopathol. 87, 137–145.
Shah, K., Rajab, A., Oldaker, T., Illingwoth, A., Taylor, A., 2021. Selection and Validation Strategy for Adding Antibodies to Flow Cytometry Panels.
Stein, R., Belisle, E., Hansen, H.J., Goldenberg, D.M., 1993. Epitope specificity of the anti-(B cell lymphoma) monoclonal antibody, LL2. Cancer Immunol. Immunother. CII 37, 293–298.
Stepanova, K., Sinkora, M., 2013. Porcine γδ T lymphocytes can be categorized into two functionally and developmentally distinct subsets according to expression of CD2 and level of TCR. J. Immunol. 190, 2111–2120.
Talker, S.C., Käser, T., Reutner, K., Sedlak, C., Mair, K.H., Koinig, H., Graage, R., Viehmann, M., Klingler, E., Ladinig, A., Ritzmann, M., Saalmüller, A., Gerner, W., 2013. Phenotypic maturation of porcine NK- and T-cell subsets. Dev. Comp. Immunol. 40, 51–68.
Tangri, S., Vall, H., Kaplan, D., Hoffman, B., Purvis, N., Porwit, A., Hunsberger, B., Shankey, T.V., 2013. Validation of cell-based fluorescence assays: practice guidelines from the ICSH and ICCS - part III - analytical issues. Cytom. Part B Clin. Cytom. 84, 291–308.
Terry, L.A., DiSanto, J.P., Small, T.N., Flomenberg, N., 1990. Differential expression and regulation of the human CD8 alpha and CD8 beta chains. Tissue Antigens 35, 82–91.
Vita, M., de, Catzola, V., Buzzonetti, A., Fossati, M., Battaglia, A., Zamai, L., Fattorossi, A., 2015. Unexpected interference in cell surface staining by monoclonal antibodies to unrelated antigens. Cytom. Part B Clin. Cytom. 88, 352–354.
Wang, M., Misakian, M., He, H.-J., Bajcsy, P., Abbasi, F., Davis, J.M., Cole, K.D., Turko, I. V., Wang, L., 2014. Quantifying CD4 receptor protein in two human CD4+ lymphocyte preparations for quantitative flow cytometry. Clin. Proteom. 11, 43.
Yang, H., Parkhouse, R.M., 1996. Phenotypic classification of porcine lymphocyte subpopulations in blood and lymphoid tissues. Immunology 89, 76–83.
Yang, H., Parkhouse, R.M., 1997. Differential expression of CD8 epitopes amongst porcine CD8-positive functional lymphocyte subsets. Immunology 92, 45–52.
Zuckermann, F.A., Pescovitz, M.D., Aasted, B., Dominguez, J., Trebichavsky, I., Novikov, B., Valpotic, I., Nielsen, J., Arn, S., Sachs, D.H., Lunney, J.K., Boyd, P., Walker, J., Lee, R., Davis, W.C., Barbosa, I.R., Saalmüller, A., 1998. Report on the analyses of mAb reactive with porcine CD8 for the second international swine CD workshop. Vet. Immunol. Immunopathol. 60, 291–303.